198571: pelitic migmatite, Dumbleyung

(Youanmi Terrane, Yilgarn Craton)

Blereau, ER, Kelsey, DE and Korhonen, FJ

Location and sampling

DUMBLEYUNG (SI 50-7), DUMBLEYUNG (2431)

MGA Zone 50, 569703E 6316611N

Warox Site FJKBGD198571

Sampled on 6 June 2010

This sample was collected from a pile of rocks in a field along Bagnalls Road, about 18.3 km southeast of Yodgabin Rock, 14.8 km south-southwest of Kasnabblin Rock and 2.9 km north of Dumbleyung. The sample was collected as part of the unpublished Yilgarn Craton Metamorphic Project (2003–14) undertaken by Ben Goscombe for the Geological Survey of Western Australia (GSWA), and referred to in that study as sample BG10-35b. The results from this project have not been released by GSWA, although select data have been published in Goscombe et al. (2019).

Tectonic unit

The unit sampled is a pelitic migmatite near the western margin of the Youanmi Terrane (Quentin de Gromard et al., 2021). This unit is part of a northwest-trending belt of Archean metasedimentary and gneissic rocks previously assigned to the South West Terrane and referred to informally by Wilde (2001) as the 'Lake Grace domain' (cf. Pidgeon et al., 2010). The boundary between the South West and Youanmi Terranes in this area is a major, northwest-trending shear zone system (Quentin de Gromard et al., 2021). A metagranodiorite, sampled from a core drilled about 32 km to the south-southeast, yielded an igneous crystallization age of 2670 ± 5 Ma, and an age of 2635 ± 5 Ma for high-grade metamorphism (GSWA 219902, Lu et al., 2020b). Another sample of metagranodiorite, collected from a core drilled about 36 km to the southeast, yielded an igneous crystallization age of 2643 ± 3 Ma (GSWA 219901, Lu et al., 2020a). Monazite from a felsic gneiss collected from the same locality as the sample reported here yielded a weighted mean $^{207}Pb/^{206}Pb$ date of 2648 ± 9 Ma, interpreted as the age of high-grade metamorphism (GSWA 198574, preliminary data).

Petrographic description

The sample is a pelitic migmatite containing approximately 40% plagioclase, 17% quartz, 17% biotite, 9% garnet, 8% K-feldspar, ~1% muscovite and pinitised cordierite and trace amounts of magnetite (Table 1, Fig. 1). The sample is heterogeneous, in that it features leucocratic layers consisting of coarser grained (up to 6 mm) plagioclase, quartz and K-feldspar, and a finer grained (up to ~1 mm) 'matrix' consisting of plagioclase with lesser amounts quartz, K-feldspar, garnet and biotite (Figs 1, 2). The leucocratic layers are interpreted to be leucosomes whereas the biotite-bearing portion of the rock is interpreted as (residual) melanosome. Garnet porphyroblasts (1–5 mm diameter) are restricted to the melanosome and are rich in quartz inclusions and lesser amounts of biotite inclusions (Fig. 2). Magnetite is also restricted to the melanosome. Rare altered equant, porphyroblastic grains of pinite are interpreted to represent altered and pseudomorphed cordierite and are located within the margin of leucosome (Figs 1, 2). Based on these observations, the interpreted peak metamorphic assemblage is garnet–plagioclase–quartz–K-feldspar–biotite–cordierite–magnetite.

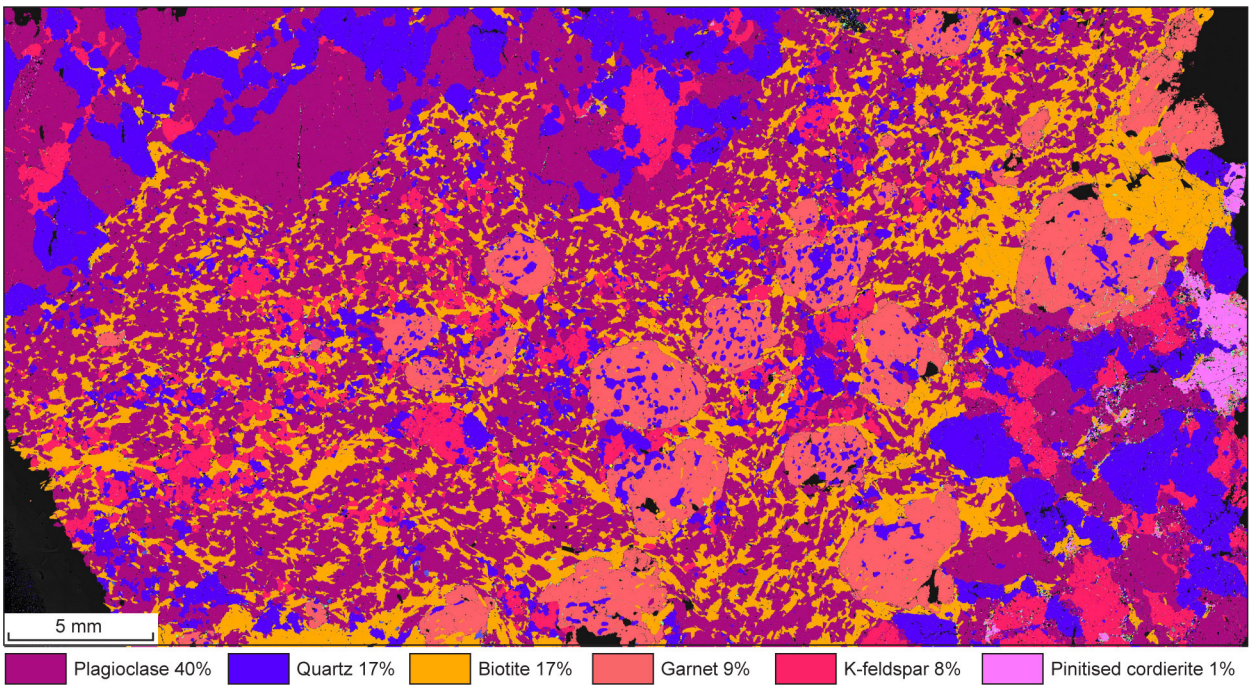

Figure 1. **TESCAN Integrated Mineral Analyser (TIMA) image of an entire thin section from sample 198571: pelitic migmatite, Dumbleyung. Volume percent proportion of major rock-forming minerals are calculated by the TIMA software**

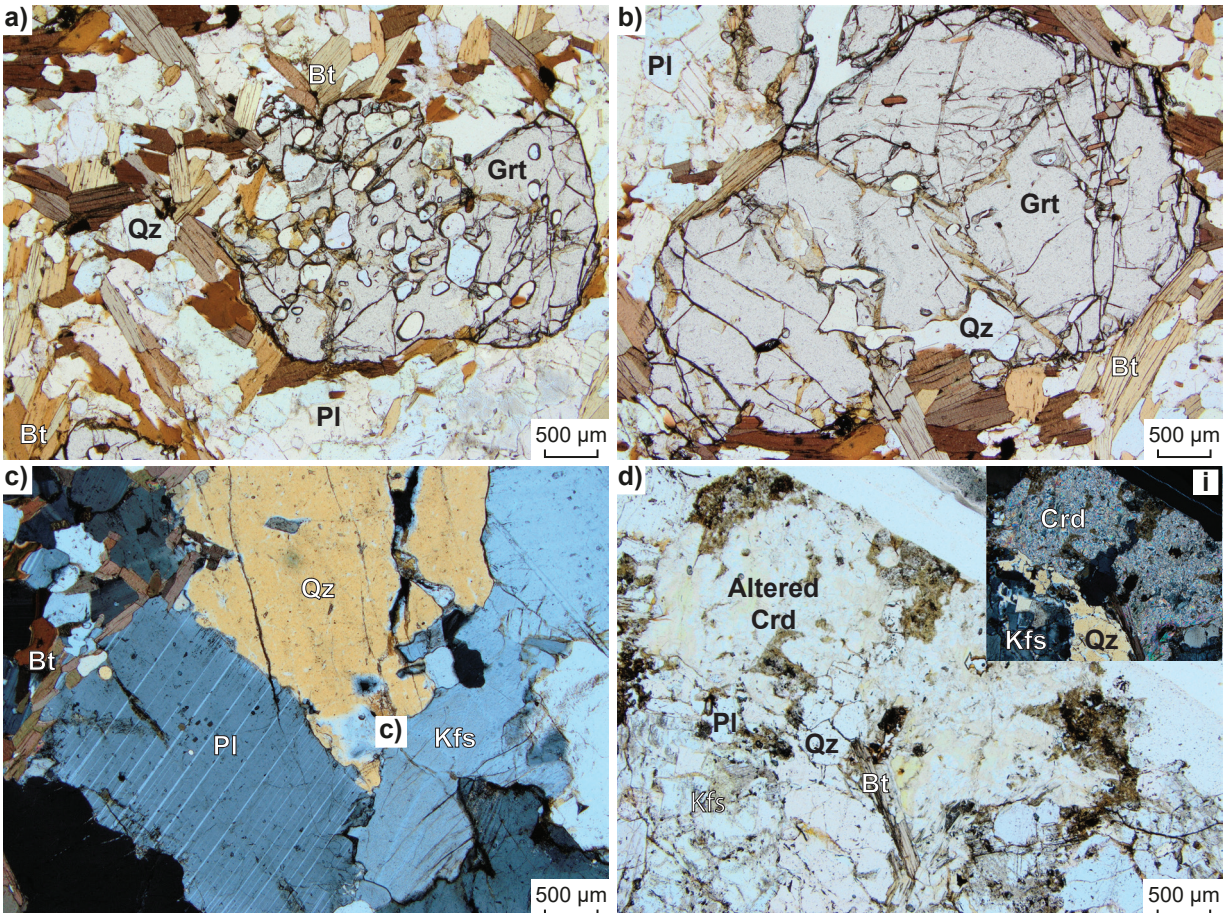

Figure 2. **Photomicrographs, in plane-polarized (a, b, d) and cross-polarised light (c), of sample 198571: pelitic migmatite, Dumbleyung. Mineral abbreviations are explained in the caption to Figure 3**

Table 1. Mineral modes for sample 198571: pelitic migmatite, Dumbleyung

Mineral modes	Pl	Qz	Bt	Grt	Kfs	Crd[(a)]	Mt	Ilm
Observed (vol%)[(b)]	40	17	17	9	8	1	<1	--
Predicted (mol%)								
@ 805 °C, 4.2 kbar	38	28	13	5	9	6	0.4	0.1
@ 845 °C, 6.8 kbar	32	23	3	16	15	0.4	--	0.8

NOTES: (a) In thin section Crd is pinitised and its former presence is inferred
(b) trace monazite and zircon also present in thin section
– not present

Methodology and analytical details

Preliminary *P–T* estimates were obtained using multiple-reaction thermobarometry calculated from the mineral compositions (Table 2; Goscombe et al., 2019). These estimates were derived from the 'averagePT' module (avPT) in the program THERMOCALC version tc325 (Powell and Holland, 1988), using the internally consistent Holland and Powell (1998) dataset.

The metamorphic evolution of this sample has subsequently been re-evaluated using phase equilibria modelling, based on the bulk rock composition (Table 3). The bulk rock composition was determined by X-ray fluorescence spectroscopy, together with loss on ignition (LOI). FeO content was analysed by titration, and Fe_2O_3 calculated by difference. The modelled O content (for Fe^{3+}) was derived using these constraints. The modelled H_2O content was constrained using a $T–M_{H2O}$ pseudosection, selecting a H_2O content of 1.84 mol% H_2O. The bulk composition was corrected for the presence of apatite by applying a correction to calcium (Table 3). Thermodynamic calculations were performed in the MnNCKFMASHTO ($MnO–Na_2O–CaO–K_2O–FeO–MgO–Al_2O_3–SiO_2–H_2O–TiO_2–O$) system using THERMOCALC version tc340 (Powell and Holland, 1988; updated October 2013) and the internally consistent thermodynamic dataset of Holland and Powell (2011; dataset tc-ds62, created in February 2012). The activity–composition relations used in the modelling are detailed in White et al. (2014a,b). Additional information on the workflow with relevant background and methodology are provided in Korhonen et al. (2020).

Table 2. Mineral compositions for sample 198571: pelitic migmatite, Dumbleyung

Mineral[a]	Pl	Pl	Pl	Pl	Bt	Bt	Bt	Bt	Grt	Grt	Grt	Grt	Kfs	Kfs
Setting[b]	Core	Rim	Core	Rim	Core	Rim	Core	Rim	Core	Mantle	Rim	OR	Core	Rim
wt%														
SiO_2	61.81	61.48	61.74	61.95	36.48	36.31	37.24	37.20	39.01	39.14	37.96	37.81	64.26	64.42
TiO_2	0.03	0.03	0.01	0.01	4.19	4.35	4.11	4.06	0.02	0.03	0.02	0.02	0.05	0.07
Al_2O_3	24.16	24.45	24.15	24.31	15.34	15.17	15.76	15.65	22.32	22.43	21.52	21.36	20.45	18.82
Cr_2O_3	0.00	0.00	0.00	0.00	0.31	0.27	0.32	0.31	0.02	0.00	0.12	0.12	0.00	0.02
FeO	0.06	0.04	0.01	0.12	14.12	13.89	13.93	13.86	27.54	28.43	30.95	31.02	0.08	0.00
MnO	0.00	0.00	0.06	0.00	0.02	0.00	0.04	0.03	0.78	0.68	1.13	1.14	0.01	0.00
MgO	0.01	0.00	0.00	0.00	14.02	13.69	14.44	14.37	10.11	9.83	7.17	6.91	0.01	0.01
ZnO	0.00	0.04	0.00	0.00	0.09	0.17	0.09	0.02	0.04	0.00	0.00	0.00	0.00	0.07
CaO	5.41	5.84	5.74	5.64	0.00	0.03	0.01	0.01	1.01	0.99	1.06	1.04	1.54	0.07
Na_2O	8.12	8.09	8.23	7.88	0.03	0.07	0.03	0.06	0.01	0.03	0.00	0.00	4.26	1.52
K_2O	0.76	0.60	0.52	0.27	10.12	9.70	9.99	9.79	0.00	0.00	0.00	0.00	9.36	14.51
Total[c]	100.37	100.56	100.46	100.17	94.71	93.65	95.97	95.36	100.87	101.58	99.93	99.43	100.01	99.50
Oxygen	8	8	8	8	11	11	11	11	12	12	12	12	8	8
Si	2.74	2.72	2.73	2.76	2.74	2.75	2.75	2.76	2.97	2.96	2.97	2.98	2.91	2.98
Ti	0.00	0.00	0.00	0.00	0.24	0.25	0.23	0.23	0.00	0.00	0.00	0.00	0.00	0.00
Al	1.26	1.27	1.26	1.27	1.36	1.36	1.37	1.37	2.00	2.00	1.99	1.99	1.09	1.02
Cr	0.00	0.00	0.00	0.00	0.02	0.02	0.02	0.02	0.00	0.00	0.01	0.01	0.00	0.00
Fe^{3+}[d]	0.00	0.00	0.00	0.00	0.04	0.04	0.04	0.04	0.07	0.02	0.00	0.04	0.00	0.00
Fe^{2+}	0.00	0.00	0.00	0.00	0.84	0.84	0.82	0.82	1.68	1.78	2.03	2.01	0.00	0.00
Mn^{2+}	0.00	0.00	0.00	0.00	0.00	0.00	0.00	0.00	0.05	0.04	0.08	0.08	0.00	0.00
Mg	0.00	0.00	0.00	0.00	1.57	1.55	1.59	1.59	1.15	1.11	0.84	0.81	0.00	0.00
Zn	0.00	0.00	0.00	0.00	0.01	0.01	0.00	0.00	0.00	0.00	0.00	0.00	0.00	0.00
Ca	0.26	0.28	0.27	0.27	0.00	0.00	0.00	0.00	0.08	0.08	0.09	0.09	0.07	0.00
Na	0.70	0.69	0.71	0.68	0.00	0.01	0.00	0.01	0.00	0.00	0.00	0.00	0.37	0.14
K	0.04	0.03	0.03	0.02	0.97	0.94	0.94	0.93	0.00	0.00	0.00	0.00	0.54	0.85
Total	5.00	5.00	5.00	5.00	7.80	7.76	7.78	7.76	8.00	8.00	8.00	8.00	5.00	5.00
Compositional variables														
XFe[e]	–	–	–	–	0.35	0.35	0.34	0.34	0.59	0.62	0.71	0.71	–	–

NOTES: – not applicable
(a) Mineral abbreviations explained in the caption to Figure 3
(b) OR, outer rim
(c) Totals on anhydrous basis
(d) Fe^{3+} contents for biotite assumed to be 10% of Fe total; Fe3+ contents for other minerals based on Droop (1987)
(e) XFe = $Fe^{2+}/(Fe^{2+} + Mg)$

Table 3. Measured whole-rock and modelled compositions for sample 198571: pelitic migmatite, Dumbleyung

XRF whole-rock composition (wt%) [a]

SiO_2	TiO_2	Al_2O_3	Fe_2O_3 [b]	FeO [c]	MnO	MgO	CaO	Na_2O	K_2O	P_2O_5	LOI	Total
65.71	0.55	16.05	6.12	4.77	0.11	2.63	2.10	3.32	2.85	0.04	0.75	100.23

Normalized composition used for phase equilibria modelling (mol%)

SiO_2	TiO_2	Al_2O_3	O [d]	FeO^T [e]	MnO	MgO	CaO [f]	Na_2O	K_2O	--	H_2O [g]	Total
70.36	0.44	10.12	0.33	4.92	0.10	4.20	2.34	3.41	1.95		1.84	100.01

NOTES: (a) Data and analytical details are available from the WACHEM database <http://geochem.dmp.wa.gov.au/geochem/>
(b) Fe_2O_3 content is total Fe
(c) FeO measured by titration
(d) O content (for Fe_2O_3) determined from Fe_2O_3T using the constraint of the FeO titration value
(e) FeO^T = moles FeO + 2 * moles O
(f) CaO modified to remove apatite: CaO(Mod) = CaO(Total) - (moles CaO(in Ap) = 3.33 * moles P_2O_5)
(g) H_2O content constrained via T–X_{H2O} pseudosection analysis

Results

Metamorphic *P–T* estimates have been derived based on detailed examination of one thin section and the bulk rock composition; care was taken to ensure that the thin section and the sample volume selected for whole-rock chemistry were similar in terms of featuring the same minerals in approximately the same abundances (Table 1), to minimize any potential compositional differences. The *P–T* pseudosection was calculated over the range 750–900 °C and 3–10 kbar (Fig. 3). The hydrated solidus is located at 770–805 °C across the range of modelled pressures. Garnet is stable above 3.0 kbar above 795 °C and 4.1 kbar at 900 °C. Sillimanite is stable above 5 kbar at 750 °C and 7 kbar at 845 °C. Magnetite is stable below 5.8 kbar across the modelled range of temperatures. Cordierite is stable below 7 kbar at 845 °C (Fig. 3).

Metamorphic *P–T* estimates (± 2σ uncertainty) calculated using multiple-reaction thermobarometry are 6.9 ± 1.1 kbar and 750 ± 27 °C (Goscombe et al., 2019). These calculations used the mineral core compositions (Table 2) to estimate peak conditions.

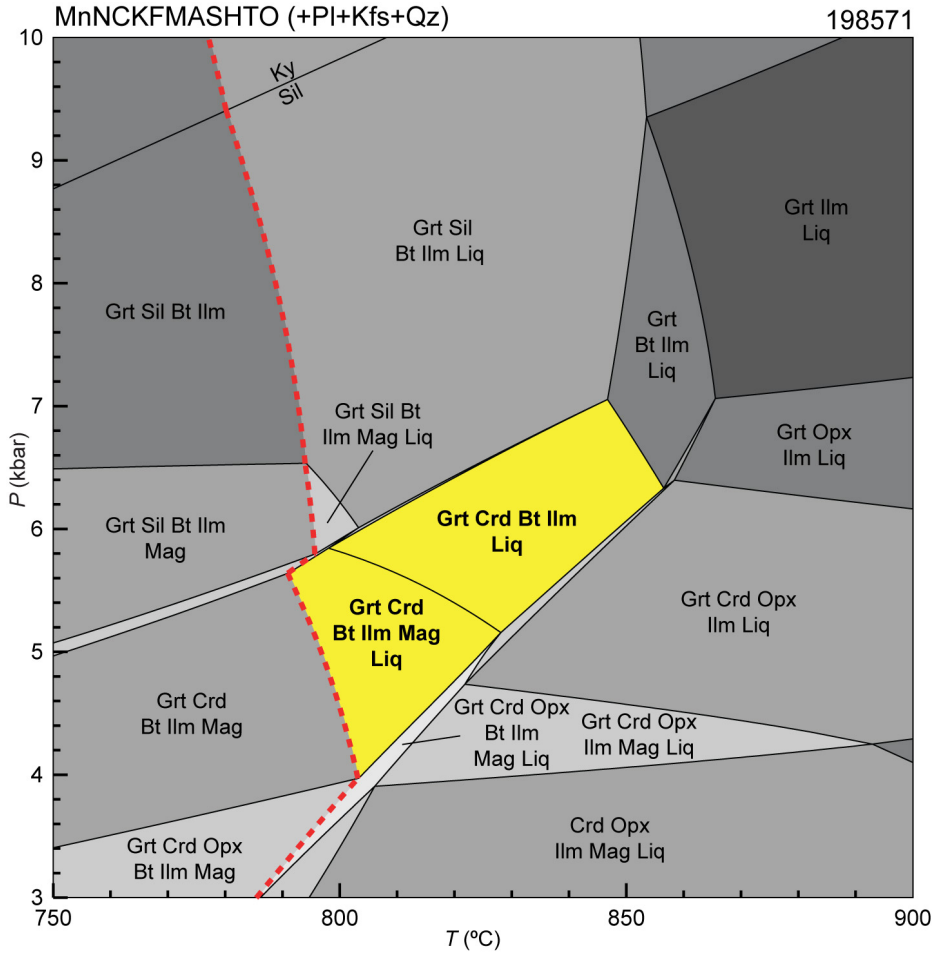

Figure 3. ***P–T*** **pseudosection calculated for sample 198571: pelitic migmatite, Dumbleyung. Assemblage fields corresponding to peak metamorphic conditions are shown in bold text and yellow shading. Red dashed line represents the solidus. Abbreviations: Bt, biotite; Crd, cordierite; Grt, garnet; Ilm, ilmenite; Kfs, K-feldspar; Ky, kyanite; Liq, silicate melt; Mag, magnetite; Opx, orthopyroxene; Pl, plagioclase; Qz, quartz; Sil, sillimanite**

Interpretation

The interpreted peak metamorphic assemblage of garnet–plagioclase–quartz–K-feldspar–biotite–cordierite–magnetite is stable between 790 and 830 °C at 4.0 – 5.8 kbar and 800 and 860 ºC at 5.2 – 7.0 kbar with and without magnetite, respectively. The peak field is limited by the occurrence of sillimanite at higher pressures, absence of magnetite and cordierite, respectively, at higher temperatures, occurrence of orthopyroxene at lower pressures, and the absence of melt at lower temperatures. No ilmenite occurs in the thin section, and its presence in the pseudosection (calculated mode <1%) may be due to the inability of the biotite activity–composition model to accommodate enough Ti. The results from conventional thermobarometry occur to considerably lower temperature than the stability fields of the peak assemblage in the pseudosection, at comparable pressures. Some coarser-grained biotite in contact with garnet porphyroblasts at the margin of melanosome may be of post-peak, retrograde origin, in which case the sample records some degree of cooling. The absence of post-peak cordierite, for example as coronas around garnet, could support a cooling-dominated interpretation. However, there is limited petrological information to constrain *P–T* path information.

Peak metamorphic conditions are estimated at 790–860 °C and 4.0 – 7.0 kbar, with an apparent thermal gradient between 120 and 200 °C/kbar.

References

Goscombe, B, Foster, DA, Blewett, R, Czarnota, K, Wade, B, Groenewald, B and Gray, D 2019, Neoarchaean metamorphic evolution of the Yilgarn Craton: a record of subduction, accretion, extension and lithospheric delamination: Precambrian Research, article no. 105441, doi:10.1016/j.precamres.2019.105441.

Holland, TJB and Powell, R 2011, An improved and extended internally consistent thermodynamic dataset for phases of petrological interest, involving a new equation of state for solids. Journal of Metamorphic Geology, vol. 29, no. 3, p. 333–383.

Lu, Y, Wingate, MTD and Smithies, RH 2020a, 219901: metagranodiorite, Dingo Hill mine; Geochronology Record 1685: Geological Survey of Western Australia, 5p.

Lu, Y, Wingate, MTD and Smithies, RH 2020b, 219902: metagranodiorite, Jinkas Hill mine; Geochronology Record 1686: Geological Survey of Western Australia, 5p.

Nemchin, AA and Pidgeon, RT 1997, Evolution of the Darling Range Batholith, Yilgarn Craton, Western Australia: a SHRIMP study: Journal of Petrology, v. 38, p. 625–649.

Pidgeon, RT, Wingate, MTD, Bodorkos, S and Nelson, DR 2010, The age distribution of detrital zircons in quartzites from the Toodyay– Lake Grace Domain, Western Australia: implications for the early evolution of the Yilgarn Craton: American Journal of Science, v. 310, p. 1115–1135.

Powell, R and Holland, TJB 1988, An internally consistent dataset with uncertainties and correlations: 3. Applications to geobarometry, worked examples and a computer program. Journal of Metamorphic Geology, vol. 6, no. 2, p. 173–204.

Quentin de Gromard, R, Ivanic, TJ, Zibra, I 2021 Interpreted bedrock geology of the southwest Yilgarn. Geological Survey of Western Australia, in Accelerated Geoscience Program abstracts 2021: Geological Survey of Western Australia, Record 2021/4.

White, RW, Powell, R, Holland, TJB, Johnson, TE and Green, ECR 2014a, New mineral activity-composition relations for thermodynamic calculations in metapelitic systems: Journal of Metamorphic Geology, v. 32, no. 3, p. 261–286.

White, RW, Powell, R and Johnson, TE 2014b, The effect of Mn on mineral stability in metapelites revisited: New a-x relations for manganese-bearing minerals: Journal of Metamorphic Geology, doi:10.1111/jmg.12095.

Wilde, SA, 2001, Jimperding and Chittering metamorphic belts, southwestern Yilgarn Craton, Western Australia — a field guide: Geological Survey of Western Australia, Record 2001/12, 24p.

Links

Metamorphic history introduction document: Intro_2020.pdf

Recommended reference for this publication

Blereau, ER, Kelsey, DE and Korhonen, FJ 2021, 198571: pelitic migmatite, Dumbleyung; Metamorphic History Record 10: Geological Survey of Western Australia, 7p.

Data obtained: 27 January 2021

Date released: 25 June 2021

This Metamorphic History Record was last modified on 9 June 2021.

Grid references in this publication refer to the Geocentric Datum of Australia 1994 (GDA94). All locations are quoted to at least the nearest 100 m.

WAROX is GSWA's field observation and sample database. WAROX site IDs have the format 'ABCXXXnnnnnnSS', where ABC = geologist username, XXX = project or map code, nnnnnn = 6 digit site number, and SS = optional alphabetic suffix (maximum 2 characters).

Isotope and element analyses are routinely conducted using the GeoHistory laser ablation ICP-MS and Sensitive High-Resolution Ion Microprobe (SHRIMP) ion microprobe facilities at the John de Laeter Centre (JdLC), Curtin University, with the financial support of the Australian Research Council and AuScope National Collaborative Research Infrastructure Strategy (NCRIS). The TESCAN Integrated Mineral Analyser (TIMA) instrument was funded by a grant from the Australian Research Council (LE140100150) and is operated by the JdLC with the support of the Geological Survey of Western Australia, The University of Western Australia (UWA) and Murdoch University. Mineral analyses are routinely obtained using the electron probe microanalyser (EPMA) facilities at the Centre for Microscopy, Characterisation and Analysis at UWA, and at Adelaide Microscopy, University of Adelaide.

Digital data related to WA Geology Online, including geochronology and digital geology, are available online at the Department's Data and Software Centre and may be viewed in map context at GeoVIEW.WA.

Further details of geoscience products are available from:
Information Centre
Department of Mines, Industry Regulation and Safety
100 Plain Street
EAST PERTH WA 6004
Telephone: +61 8 9222 3459 | Email: publications@dmirs.wa.gov.au
www.dmirs.wa.gov.au/GSWApublications